Chapter

Comparison and Analysis of Diffusion Models for the Fe_2B Layers Formed on the AISI 12L14 Steel by Using Powder-Pack Technique

Martín Ortiz Domínguez

Abstract

Boriding is a thermochemical surface treatment, a diffusion process similar to carburizing and nitriding in that boron is diffused into a metal base. An indispensable tool to choose the suitable process parameters for obtaining boride layer of an adequate thickness is the modeling of the boriding kinetics. Moreover, the simulation of the growth kinetics of boride layers has gained great interest in the recent years. In this chapter, the AISI 12L14 steel was pack-borided in the temperature range of 1123–1273 K for treatment times between 2 and 8 h. A parabolic law for the kinetics of growth of Fe_2B layers formed on the surface of AISI 12L14 steel was deducted. Two diffusion models were proposed for estimating the boron diffusion coefficients through the Fe_2B layers. The measurements of the thickness (Fe_2B), for different temperature of boriding, were used for calculations. As a result, the boron activation energy for the AISI 12L14 steel was estimated as 165.0 kJ/mol. In addition, to extend the validity of the present models, two additional boriding conditions were done. The Fe_2B layers grown on AISI 12L14 steel were characterized by use of the following experimental techniques: X-ray diffraction, scanning electron microscopy and energy dispersive X-ray spectroscopy.

Keywords: diffusion model, activation energy, parabolic growth law, diffusion coefficient, growth kinetics

1. Introduction

Surface hardening of steel can be achieved, mainly through two procedures: modifying the chemical composition of the surface by diffusion of some chemical element (carbon, nitrogen, boron, sulfur, etc.) in which case it is known as thermochemical treatment (**Table 1**) or modifying only the microstructure of the surface by thermal treatment, then known as surface treatment. The current technological demands highlight the need to have metallic materials with high performance under critical service conditions, consequently, the increase in the wear resistance, preserving its ductility and the toughness of the core.

According to **Table 1**, there are three methods of surface hardening:

- Diffusion process that modifies the chemical composition where a component in a solid mixture can diffuse through another at a speed is measurable, if there is a suitable concentration gradient and the temperature is high enough. The effects of diffusion in solids are very important in metallurgy (increase surface hardness) as well: The continuous flux of carbon, nitrogen, boron, and so on, can form a hard coating, where the mass transfer is described by Fick's laws.

- Applied energy process, the interesting about these processes is that it is not necessary to incorporate any element to the substrate. For example, tempering is a heat treatment in which steel is heated up to austenization temperatures and subsequently it is cooled rapidly, with in order to obtain a transformation that provides a structure martensitic hard and resistant. Surface tempering is generally used to components that need a hard surface and a substrate with a high value of fracture toughness.

- Coating and surface hardness, the coating covers the surface of the substrate, obtained after the deposition process, substrates considerably increase the physical characteristics of hardness and corrosion resistance, maintaining the original morphological characteristics (roughness and brilliance) unchanged, making the functional and decorative coating at the same time.

The current technological requirements highlight the need to have metallic materials with specific characteristics, for increasingly critical service conditions. For example, the metal dies used in the metallurgical processes of cold working and hot metals need a high toughness and surface hardness, especially at high temperature. Surface hardening of steel can be achieved, basically, by two processes: modifying the chemical composition of the surface by diffusion of some chemical elements (carbon, nitrogen, sulfur, boron, aluminum, zinc, chromium, and so on). Only boriding process for surface hardening is briefly reviewed in this chapter, boriding is a thermochemical treatment in which boron atoms are diffused into the surface of a workpiece and form borides with the base metal. Apart from constructional materials, which meet these high demands, processes have been developed which have a positive effect on the tribological applications including abrasive, adhesive, fatigue and corrosion wear of the component surface [1–3]. Boride layers are of particular benefit when the components have to withstand abrasive wear. The fundamental advantage of the borided layers (FeB and Fe_2B) is that they can reach high hardness near the surface (1800 $HV_{0.1}$ and 2000 $HV_{0.1}$), maintained at high temperatures [4–8]. In this chapter, the growth kinetics of single phase layer (Fe_2B)

Diffusion methods	Applied energy methods	Coating and surface modification
Carburizing	Flame hardening	Hard chromium planting
Nitriding	Induction hardening	Electroless nickel plating
Carbonitriding	Laser beam hardening	Thermal spraying
Boriding	Electron beam hardening	Weld hardfacing
Thermal diffusion process		Chemical vapor deposition
		Physical vapor deposition
		Ion implantation
		Laser surface processing

Table 1.
Engineering methods for surface hardening of steels.

on the ferrous substrate was studied during the iron powder-pack boriding (steady state and non-steady state). The parabolic growth law for the borided layers was mathematically estimated. Likewise, a mass balance equation was proposed at the Fe_2B/substrate (AISI 12L14) interface. Moreover, the boron diffusion coefficients (D_{Fe_2B}) in the Fe_2B layers were determined considering two mathematical models for mass transfer. The Fe_2B layers formed on the alloy surface is controlled by the diffusion of boron atoms, and the presence of the Fe_2B layers was checked by the XRD technique. Finally, the distribution of the alloy elements in AISI 12L14 borided steel was verified by chemical microanalysis technique (EDS) used in conjunction with SEM.

1.1 The diffusion models

One of the most important parameters that characterizes the Fe_2B layers is the thickness, since the properties of the coating depend on it, such as: resistance to wear, fatigue, hardness, and dynamic loads, as well as to a large extent determining the grip with the substrate. Having an expression that allow estimating the layer thickness during the boriding process, facilitates the appropriate selection of the technological parameters, in order to guarantee the desired properties. The layer thickness exhibits a time dependence such that:

$$\text{layer thickness v} \approx t^{1/2}, \tag{1}$$

1.1.1 Derivation of the parabolic growth law

In diffusion processes, parabolic kinetics occurs when the mass gain on a sample is proportional to the square root of time. In general, parabolic kinetics indicates that diffusion of reactants (such as boron) through a growing layer is rate-determining. If the diffusion of B atoms is rate-determining, the layer rate is proportional to the flux through the substrate:

$$\frac{dx}{dt} \approx J_{Fe_2B}(x,t). \tag{2}$$

El flux, $J_{Fe_2B}(x,t)$, can be written as

$$J_{Fe_2B}(x,t) = C_{Fe_2B}(x,t)(dx/dt), \tag{3}$$

where $C_{Fe_2B}(x,t)$ is the boron concentration profile in mol/m^3 and is the velocity dx/dt of Fe_2B layer in m/s, $J_{Fe_2B}(x,t)$ giving units of mol/m^2 s. The velocity of a particle is proportional to the force, F, on the particle:

$$dx/dt = B_{Fe_2B}F, \tag{4}$$

where B_{Fe_2B} is the mobility of the boron. Writing the chemical potential as μ_{Fe_2B}, this force is written as

$$F = -\partial\mu_{Fe_2B}/\partial x, \tag{5}$$

for a Fe_2B layer with thickness x. Combining Eq. (4) and (5) yields

$$J_{Fe_2B}(x,t) = -C_{Fe_2B}(x,t)B_{Fe_2B}\partial\mu_{Fe_2B}/\partial x, \tag{6}$$

from the relationship

$$\mu_{Fe_2B} = \mu^o_{Fe_2B} + k_B T \ln a_{Fe_2B}, \tag{7}$$

where k_B is the Boltzmann's constant, we can write

$$\frac{\partial \mu_{Fe_2B}}{\partial x} = \frac{\partial\left(\mu^o_{Fe_2B} + k_B T \ln a_{Fe_2B}\right)}{\partial x} = k_B T \frac{\partial \ln a_{Fe_2B}}{\partial x}. \tag{8}$$

In an ideal system, the concentration, $C_{Fe_2B}(x,t)$, is equivalent to activity, $a_{Fe_2B}(x,t)$. Substituting the Eq. (8) into Eq. (6), we get

$$J_{Fe_2B}(x,t) = -C_{Fe_2B}(x,t) B_{Fe_2B} k_B T \frac{\partial \ln C_{Fe_2B}(x,t)}{\partial x} = -B_{Fe_2B} k_B T \frac{\partial C_{Fe_2B}(x,t)}{\partial x}. \tag{9}$$

As shown in Eq. (2),

$$\frac{dx}{dt} = (\text{constant}) J_{Fe_2B}(x,t), \tag{10}$$

so that a combination of Eqs. (2) and (9) gives

$$\frac{dx}{dt} = -(\text{constant}) B_{Fe_2B} k_B T \frac{\partial C_{Fe_2B}(x,t)}{\partial x}. \tag{11}$$

If we assume that the potential is fixed at each boundary of the Fe_2B layer, we can replace $\partial C_{Fe_2B}(x,t)/\partial x$ in Eq. (11) with the slope ($= \Delta C_{Fe_2B}/x$). We then introduce the parabolic growth constant k_{Fe_2B}, and set:

$$k_{Fe_2B} = -(\text{constant}) B_{Fe_2B} k_B T \Delta C_{Fe_2B}. \tag{12}$$

Combining Eqs. (11) and (12) then gives

$$\frac{dx}{dt} = \frac{k_{Fe_2B}}{x}. \tag{13}$$

Eq. (13) can be rewritten as

$$x dx = k_{Fe_2B} dt. \tag{14}$$

Upon integration of Eq. (14),

$$\int_{x=0}^{x=\mathrm{v}} x dx = k_{Fe_2B} \int_{t=0}^{t=t} dt. \tag{15}$$

We arrive at the parabolic growth law:

$$\mathrm{v}^2 = 2 k_{Fe_2B} t. \tag{16}$$

1.1.2 Steady state diffusion model

Steady state means that there will not be any change in the composition profile with time. A linear boron concentration profile is considered along the depth of the Fe_2B layer as depicted in **Figure 1**. The $f(x)$ represents to the boron distribution in the substrate before the nucleation of iron boride layers on AISI 12L14 steel. $t_0^{Fe_2B}$ is

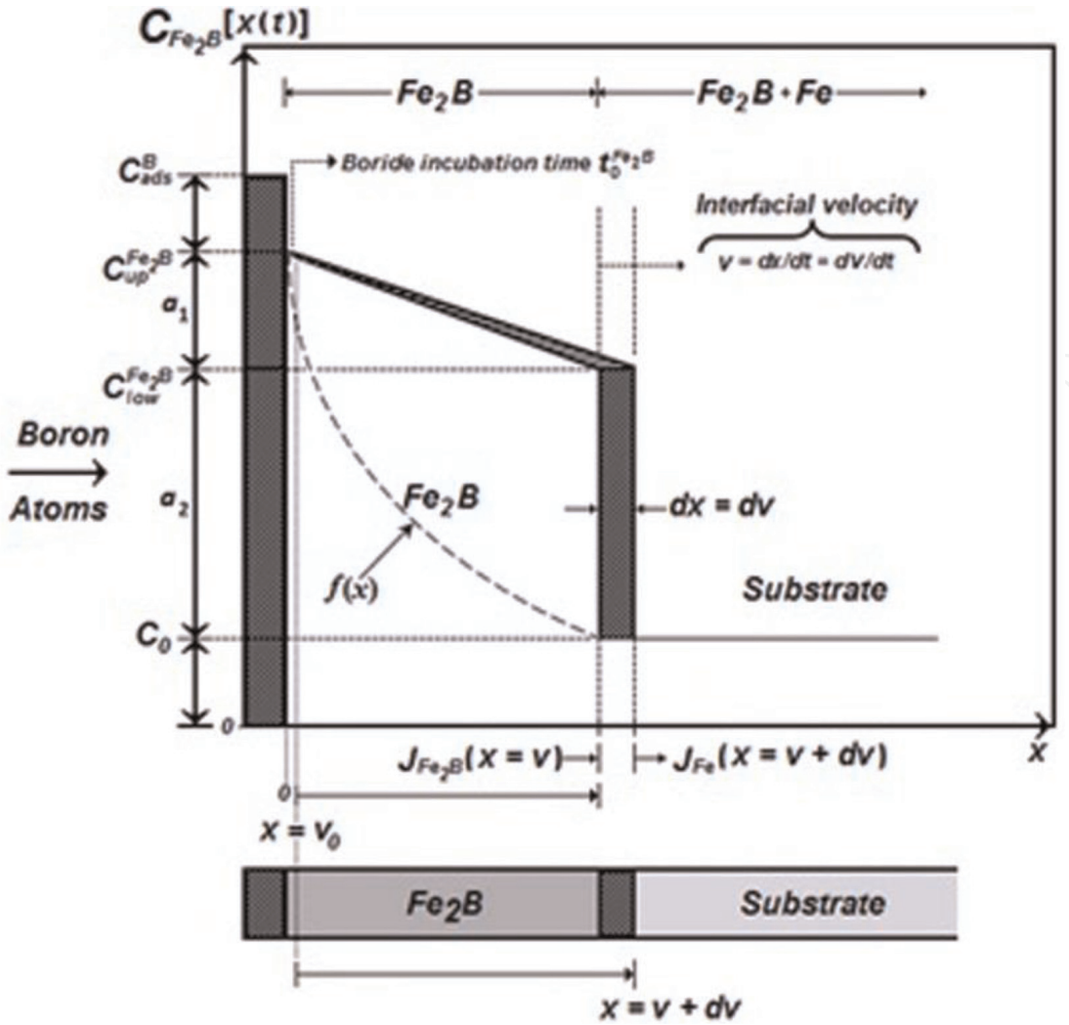

Figure 1.
A schematic linear concentration profile of boron through the Fe_2B layer is used to describe the steady state diffusion model.

the boride incubation time indispensable to form the Fe_2B phase. Moreover, $C_{up}^{Fe_2B}$ represents the boron concentration on the surface in Fe_2B layer ($= 60 \times 10^3$ molm^{-3}), $C_{low}^{Fe_2B}$ represents the boron concentration at the Fe_2B/substrate interface ($= 59.8 \times 10^3$ molm^{-3}) and $x(t = t) = v$ is the layer thickness of the boride layer (m) [9, 10].

The term C_{ads}^{B} is the effective adsorbed boron concentration during the boriding process [11]. From **Figure 1**, $a_1 = C_{up}^{Fe_2B} - C_{low}^{Fe_2B}$ defines the homogeneity range of the Fe_2B layer, $a_2 = C_{low}^{Fe_2B} - C_0$ represents the range of miscibility and C_0 is the boron concentration in the substrate (AISI 12L14) assumed as null [10, 12, 13]. During the establishment of the steady-state diffusion model, a linear concentration-profile of boron along the Fe_2B layer is considered. Likewise, the assumptions proposed by Campos-Silva et al. [8], are taken account.

v_0 is the first boride layer formed on the surface of the substrate (ASI 12 L14) during the boride incubation time [14], its thickness is very small in magnitude compared to the thickness of the boride layer (v). Moreover, regarded the mass balance equation at the growth interface (Fe_2B/substrate), which is described as follows [15–18]:

$$\left(\frac{C_{up}^{Fe_2B} + C_{low}^{Fe_2B} - 2C_0}{2}\right)\left.\frac{dx(t)}{dt}\right|_{x(t)=v} = -\left. D_{Fe_2B}\frac{\partial C_{Fe_2B}[x(t=t), t=t]}{\partial x}\right|_{x(t)=v}. \quad (17)$$

When the concentration field is independent of time and D_{Fe_2B} is independent of $C_{Fe_2B}(x,t)$, Fick's second law is reduced to Laplace's equation,

$$\nabla^2 C_{Fe_2B}[x(t)] = \frac{d^2 C_{Fe_2B}[x(t)]}{dx^2} = 0. \tag{18}$$

By solving Eq. (18), and applying the boundary conditions proposed in **Figure 1**, the distribution of boron concentration in Fe_2B is expressed as:

$$C_{Fe_2B}[x(t)] = \frac{C_{low}^{Fe_2B} - C_{up}^{Fe_2B}}{\mathrm{v}} x + C_{up}^{Fe_2B}. \tag{19}$$

By substituting the derivative of Eq. (19) with respect of the distance $x(t)$ into Eq. (17), we have

$$\left(\frac{C_{up}^{Fe_2B} + C_{low}^{Fe_2B} - \ 2C_0}{2}\right)\frac{d\mathrm{v}}{dt} = \ D_{Fe_2B}\frac{C_{up}^{Fe_2B} - C_{low}^{Fe_2B}}{\mathrm{v}}, \tag{20}$$

for $0 \le x \le \mathrm{v}$.
By substituting Eq. (16) into Eq. (20)

$$D_{Fe_2B} = \frac{1}{2}\left(\frac{C_{up}^{Fe_2B} + C_{low}^{Fe_2B} - \ 2C_0}{C_{up}^{Fe_2B} - C_{low}^{Fe_2B}}\right)k_{Fe_2B} \tag{21}$$

1.1.3 Non-steady state diffusion model in one dimension

The general diffusion equation for one-dimensional analysis under non-steady state condition is defined by Fick's second law. The growth of single phase layer (Fe_2B) with one diffusing element (boron) is observed as illustrated in **Figure 2**.

The $f(x,t)$ function represents the boron distribution in the ferritic matrix before the nucleation of Fe_2B phase as a function of time. Likewise, for analysis, the kinetic model is imposing the same restrictions as in the previous model, except the last one, it is replaced by:

- The concentration-profile of boron is the solution of the Fick's second law and depends on initial and boundary conditions through the Fe_2B zone.

The mass balance equation at the (Fe_2B/substrate) interface can be formulated by Eq. (22) as follows:

$$\left(\frac{C_{up}^{Fe_2B} + C_{low}^{Fe_2B} - \ 2C_0}{2}\right)\frac{dx(t)}{dt}\bigg|_{x(t)=\mathrm{v}} = - \ D_{Fe_2B}\frac{\partial C_{Fe_2B}[x(t=t),t=t]}{\partial x}\bigg|_{x(t)=\mathrm{v}}. \tag{22}$$

Fick's second law, isotropic one-dimensional diffusion, D_{Fe_2B} independent of concentration:

$$\frac{\partial C_{Fe_2B}[x(t),t]}{\partial t} = D_{Fe_2B}\frac{\partial^2 C_{Fe_2B}[x(t),t]}{\partial x^2}. \tag{23}$$

By solving Eq. (23), and applying the boundary conditions proposed in **Figure 2**, the boron concentration profile in Fe_2B is expressed by Eq. (24), if the boron diffusion coefficient (D_{Fe_2B}) in Fe_2B is constant for a particular temperature:

$$C_{Fe_2B}[x(t),t] = C_{up}^{Fe_2B} + \frac{C_{low}^{Fe_2B} - C_{up}^{Fe_2B}}{erf\left(\frac{v}{2\sqrt{D_{Fe_2B}t}}\right)} erf\left(\frac{x}{2\sqrt{D_{Fe_2B}t}}\right). \tag{24}$$

By substituting Eq. (24) into Eq. (22), Eq. (25) is obtained:

$$\left(\frac{C_{up}^{Fe_2B} + C_{low}^{Fe_2B} - 2C_0}{2}\right)\frac{dv}{dt} = \sqrt{\frac{D_{Fe_2B}}{\pi t}}\frac{C_{up}^{Fe_2B} - C_{low}^{Fe_2B}}{erf\left(\frac{v}{2\sqrt{D_{Fe_2B}t}}\right)} \exp\left(-\frac{v^2}{4D_{Fe_2B}t}\right), \tag{25}$$

for $0 \le x \le v$.

Substituting the expression of the parabolic growth law obtained from Eq. (16) ($v = \sqrt{2k_{Fe_2B}t}$) into Eq. (25), we have

$$\left(\frac{C_{up}^{Fe_2B} + C_{low}^{Fe_2B} - 2C_0}{4}\right)(2k_{Fe_2B})^{1/2} = \sqrt{\frac{D_{Fe_2B}}{\pi}}\frac{C_{up}^{Fe_2B} - C_{low}^{Fe_2B}}{erf\left(\sqrt{\frac{k_{Fe_2B}}{2D_{Fe_2B}}}\right)} \exp\left(-\frac{k_{Fe_2B}}{2D_{Fe_2B}}\right). \tag{26}$$

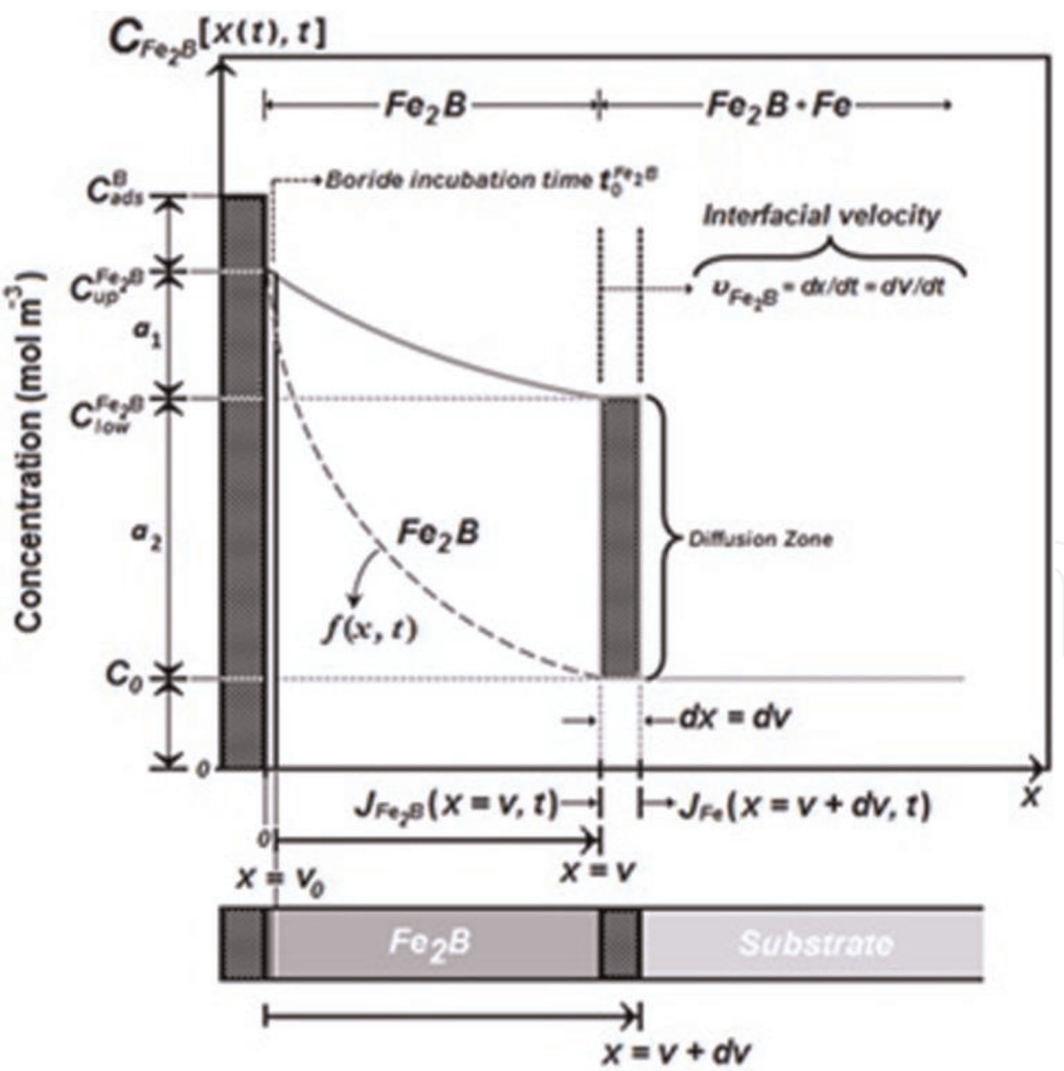

Figure 2.
A schematic non-linear concentration profile of boron through the Fe_2B layer is used to describe the non-steady state diffusion model in on dimension.

The diffusion coefficient (D_{Fe_2B}) can be estimated numerically by the Newton–Raphson method. It is assumed that expressions $C_{up}^{Fe_2B}$, $C_{low}^{Fe_2B}$, and C_0, do not depend significantly on temperature (in the considered temperature range) [10].

1.2 Materials and methods

1.2.1 Powder pack boriding process

AISI 12L14 steel was used for investigation. It had a nominal chemical composition of 0.10–0.15% C, 0.040–0.090% P, 0.15–0.35% Pb, 0.80–1.20% Mn, 0.25–0.35% S, 0.10% Si. The typical applications are: brake hose ends, pulleys, disc brake pistons, wheel nuts and inserts, control linkages, gear box components (case hardened), domestic garbage bin axles, concrete anchors, padlock shackles, hydraulic fittings, vice jaws (case hardened). The samples were sectioned into cubes with dimensions of 10 mm × 10 mm × 10 mm. Prior to the boriding process, the samples were polished with SiC sandpaper up 2500 grade, ultrasonically cleaned in an alcohol solution and deionized water for 15 min at room temperature, and dried and stored under clean-room conditions. The mean hardness was 237 HV. The samples were embedded in a closed cylindrical case (AISI 316L) as shown in **Figure 3**, using Ekabor 2 as a boron-rich agent.

The powder-pack boriding process was performed in a conventional furnace under a pure argon atmosphere. It is important to note that oxygen-bearing compounds adversely affect the boriding process [1]. The thermochemical treatment

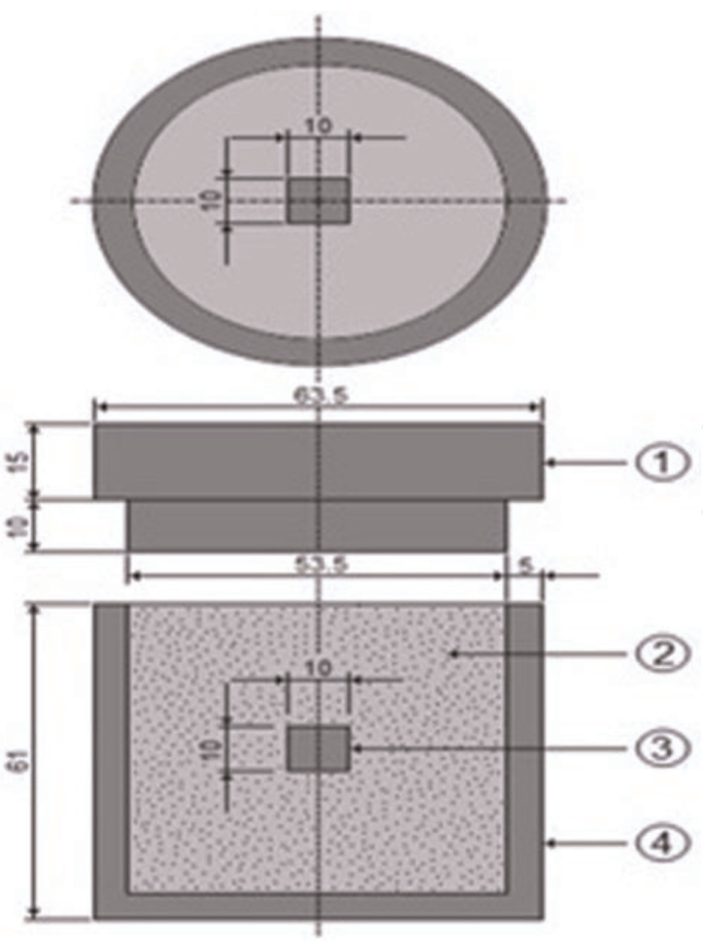

Figure 3.
Schematic view of the stainless steel AISI 304L container for the pack-powder boriding treatment (1: lid; 2: powder boriding medium (B_4C + KBF_4 + SiC); 3: sample; 4: container) (millimeter scale).

was performed at temperatures of 1123, 1173, 1223, and 1273 K with 2, 4, 6 and 8 h of exposure time. When the boriding process was concluded, the steel container was removed from the heating furnace and placed in a room temperature.

1.2.2 Characterization of boride layers

The borided samples were prepared metallographically for their characterization using GX51 Olympus equipment. As a result of preliminary experiments it was estimated that boriding started at approximately $t_0^{Fe_2B} = 29.55$ min after transferring the sample to the furnace; after that, the so-called boride incubation time sets in. The borided and etched samples were cross-sectioned, for microstructural investigations, to be observed by scanning electron microscope. The equipment used was the Quanta 3D FEG-FEI JSM7800-JOEL. **Figure 4** shows the cross-sections of boride layers formed on the surfaces of AISI 12L14 steel at different exposure times (2, 4, 6 and 8 h) and for 1173 K of boriding temperature.

The resultant microstructure of Fe_2B layers appears to be very dense and homogenous, exhibiting a sawtooth morphology where the boride needles with different lengths penetrate into the substrate [19, 20]. These elements tend to concentrate in the tips of boride layers, reducing the boron flux in this zone. The Fe_2B crystals preferably grow along the crystallographic direction [0 0 1], because it is the easiest path for the diffusion of boron in the body-centered tetragonal lattice of the Fe_2B phase [19].

It is seen that the thickness of Fe_2B layer increased with an increase of the boriding temperature (**Figure 4**) since the boriding kinetics is influenced by the

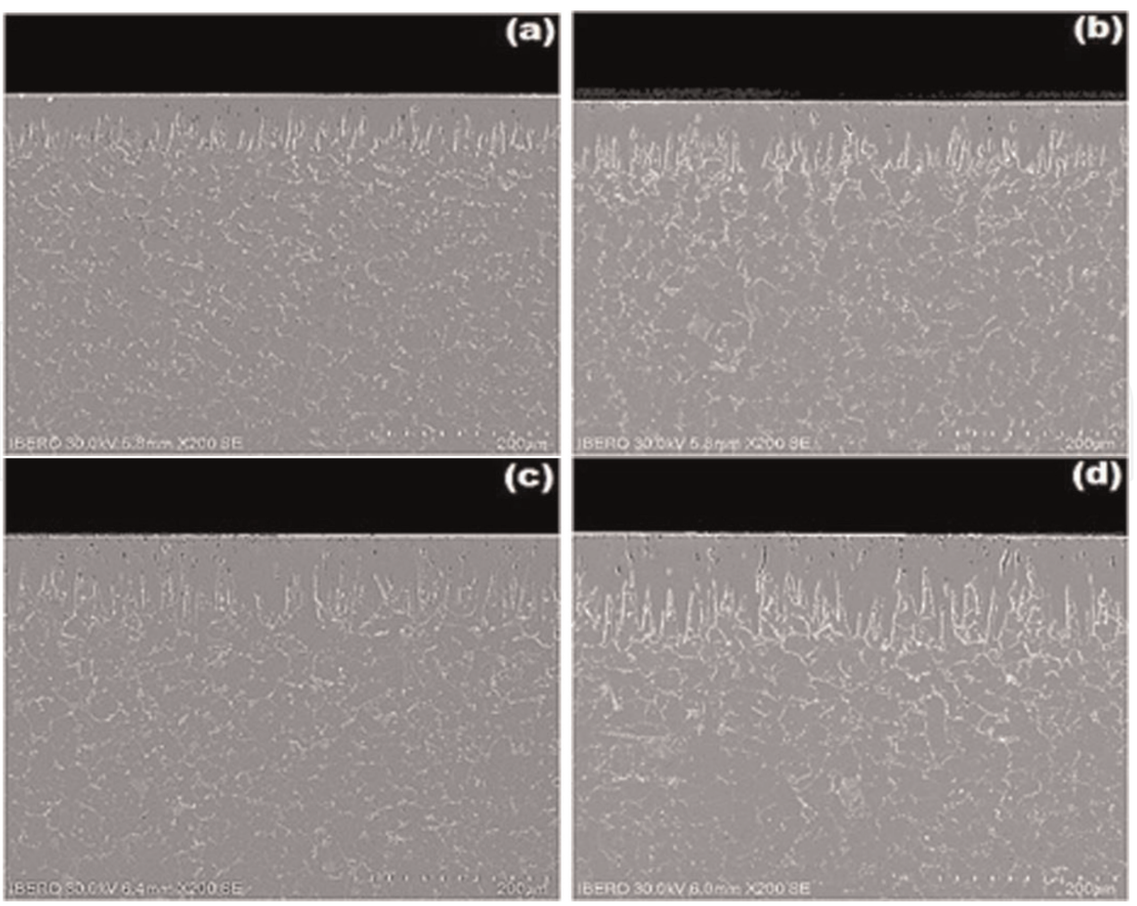

Figure 4.
SEM micrographs of the cross-sections of AISI 12L14 steel samples borided at 1173 K during different exposure times: (a) 2, (b) 4, (c) 6, and (d) 8 h.

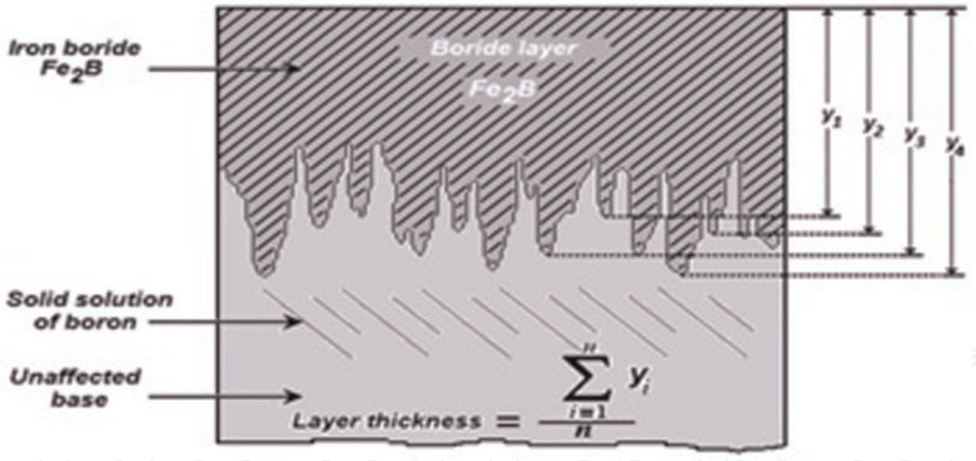

Figure 5.
Schematic diagram illustrating the procedure for estimation of boride layer thickness in AISI 12L14 steel.

treatment time. To estimate the boride layer thickness, 50 measurements were made from the surface to the long boride teeth in different sections, as shown in **Figure 5**; the boride layer thickness was measured using specialized *software* [20–22].

The identification of phases was carried out on the top surface of borided sample by an X-ray diffraction (XRD) equipment (Equinox 2000) using CoK_α radiation of 0.179 nm wavelength. In addition, the elemental distribution of the transition elements within the cross-section of boride layer was determined by electron dispersive spectroscopy (EDS) equipment (Quanta 3D FEG-FEI JSM7800-JOEL) from the surface.

1.3 Results and discussions

1.3.1 SEM observations and EDS analysis

The metallography of coating/substrate formed in AISI 12L14 borided steel at different exposure times (2, 4, 6 and 8 h) and for 1173 K of boriding temperature are shown in **Figure 4**. The EDS analysis obtained by SEM is shown in **Figure 6(a)** and **(b)**.

The results show in **Figure 6(a)** that the sulfur can be dissolve in the Fe_2B phase, in fact, the atomic radiuses of S (= 0.088 nm) is smaller than that of Fe (= 0.156 nm), and it can then be expected that S dissolved on the Fe sublattice of the borides. In **Figure 6(b)**, the resulting EDS analyses spectrums revealed that the manganese, carbon and silicon do not dissolve significantly over the Fe_2B phase and they do not diffuse through the boride layer, being displaced to the diffusion zone, and forms together with boron, solid solutions [10, 23, 24]. On boriding carbon is driven ahead of the boride layer and, together with boron, it forms borocementite, $Fe_3(B, C)$ as a separate layer between Fe_2B and the matrix with about 4 mass% B corresponding to $Fe_3(B_{0.67}C_{0.33})$ [10]. Thus, part of the boron supplied is used for the formation of borocementite. Likewise, silicon forming together with boron, solid solutions like silicoborides ($FeSi_{0.4}B_{0.6}$ and Fe_5SiB_2) [24].

1.3.2 X-ray diffraction analysis

Figure 7 shows the XRD pattern recorded on the surface of borided AISI 12L14 steel at a temperatures of: 1123 K for a treatment time of 2 h, and 1273 K for a treatment time of 8 h. The patterns of X-ray diffraction (see **Figure 7**) show the

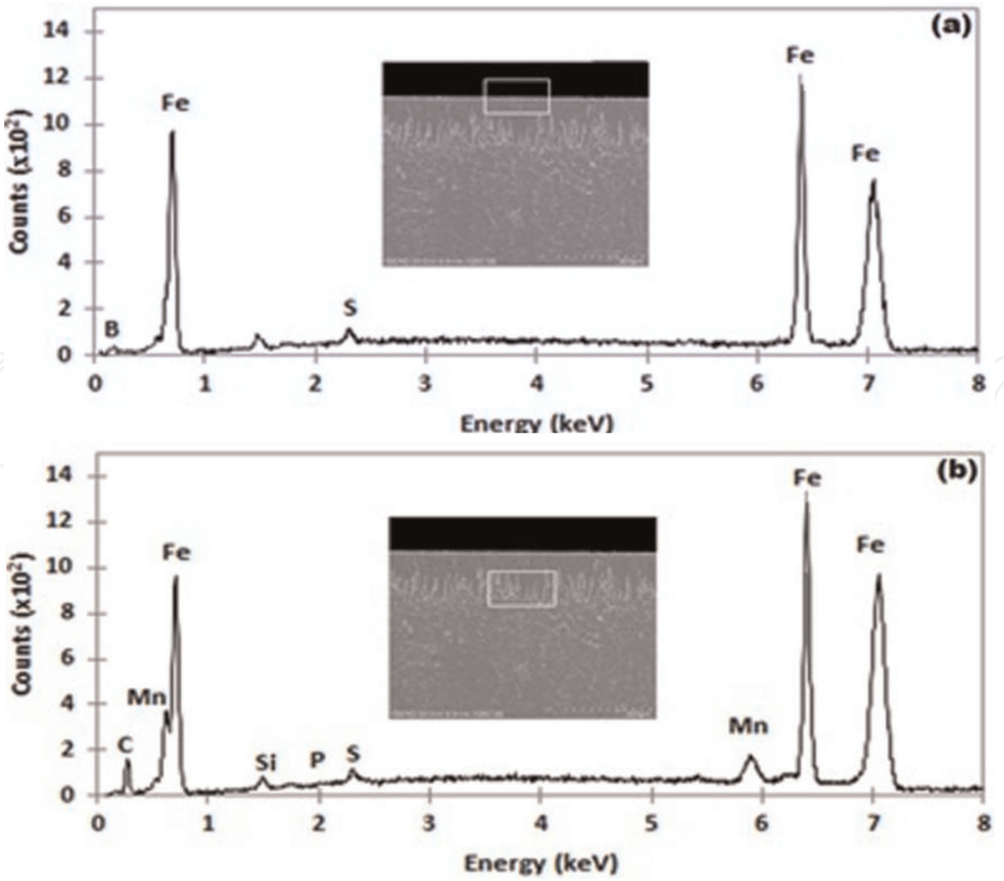

Figure 6.
A SEM micrographs of the cross-sections of the borided AISI 12L14 steel micrograph image of microstructure of the AISI 12L14 boride layer obtained at 1173 K with exposure time of 8 h, (a) and (b) EDS spectrum of borided sample.

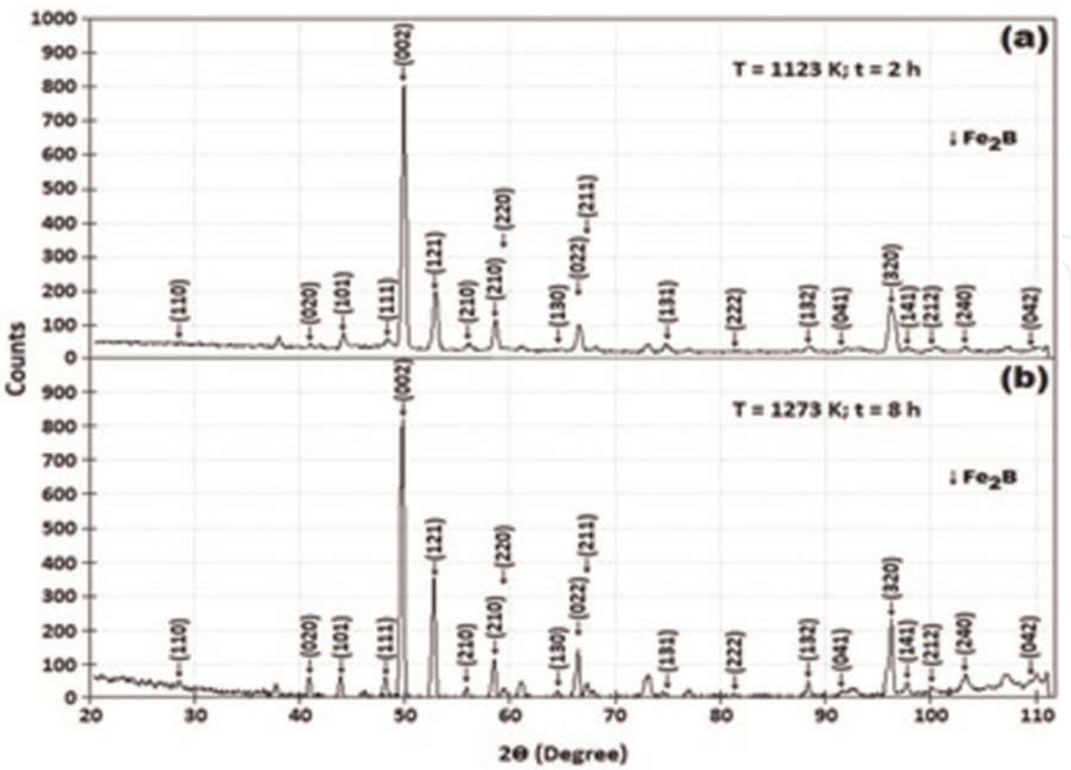

Figure 7.
XRD patterns obtained at the surface of borided AISI 12L14 steels for two boriding conditions: (a) 1123 K for 2 h and (b) 1273 K for 8 h.

presence of Fe_2B phase which is well compacted. Likewise, the patters show that there is a preferential orientation in the crystallographic plane (0 0 2) whose strength increases as the depth of the analysis increases. In a study by Martini et al. [18], the growth of the iron borides (Fe_2B) near at the Fe_2B/substrate interface only shows the diffraction peak of Fe_2B in the crystallographic plane (002).

1.3.3 Estimation of boron activation energy with steady state model

The growth kinetics of Fe_2B layers formed on the AISI 12L14 steel was used to estimate the boron diffusion coefficient through the Fe_2B layers by applying the suggested steady state diffusion model. In **Figure 8** is plotted the time dependence of the squared value of Fe_2B layer thickness for different temperatures.

In **Figure 8**, the square of boride layer thicknesses were plotted vs. the treatment time, the slopes of each of the straight lines provide the values of the parabolic growth constants ($= 2k_{Fe_2B}$). In addition, to determinate the boride incubation time, was necessary extrapolating the straight lines to a null boride layer thickness (see **Figure 8**). **Table 2** provides the estimated value of growth constants in Fe_2B at each temperature. The results, which are summarized in **Table 2**, reflect a diffusion-controlled growth of the boride layers.

In **Table 2**, the boron diffusion coefficient in the Fe_2B layers (D_{Fe_2B}) was estimated for each boriding temperature. So, an Arrhenius equation relating the boron diffusion coefficient to the boriding temperature can be adopted.

As a consequence, the boron activation energy (Q_{Fe_2B}) and pre-exponential factor (D_0) can be calculated from the slopes and intercepts of the straight line shown in coordinate system: lnD_{Fe_2B} as a function of reciprocal boriding temperature, it is presented in **Figure 9**. The boron diffusion coefficient through Fe_2B layers was deducted by steady state diffusion model as:

$$D_{Fe_2B} = 2.444 \times 10^{-3} \exp\left(-165.0329\, kJmol^{-1}/RT\right) \quad \left[m^2 s^{-1}\right]. \tag{27}$$

where: $R = 8.3144621\ \left[Jmol^{-1}K^{-1}\right]$ and T absolute temperature [K]. From the Eq. (27), the pre-exponential factor $\left(D_0 = 2.444 \times 10^{-3}\, m^2/s\right)$ and the activation

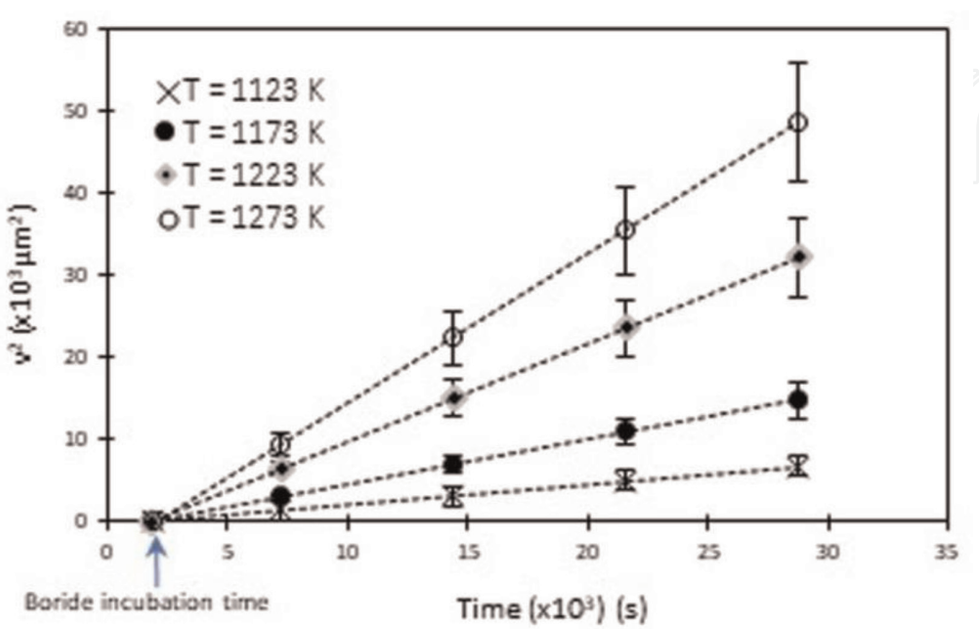

Figure 8.
Averaged squares of the Fe_2B layers (v^2) vs. boriding time (t) at different temperature.

Temperature (K)	Type of layer	Growth constants $2k_{Fe_2B}$ ($m^2\ s^{-1}$)	$D_{Fe_2B} = \frac{1}{2}\left(\frac{C_{up}^{Fe_2B}+C_{low}^{Fe_2B}-2C_0}{C_{up}^{Fe_2B}-C_{low}^{Fe_2B}}\right)k_{Fe_2B}$ Eq. (21) ($m^2\ s^{-1}$)
1123	Fe_2B	2.91×10^{-13}	5.13×10^{-11}
1173		6.12×10^{-13}	1.08×10^{-10}
1223		1.291×10^{-12}	2.27×10^{-10}
1273		2.29×10^{-12}	4.04×10^{-10}

Table 2.
The growth constants and boron diffusion coefficients as a function of boriding temperature.

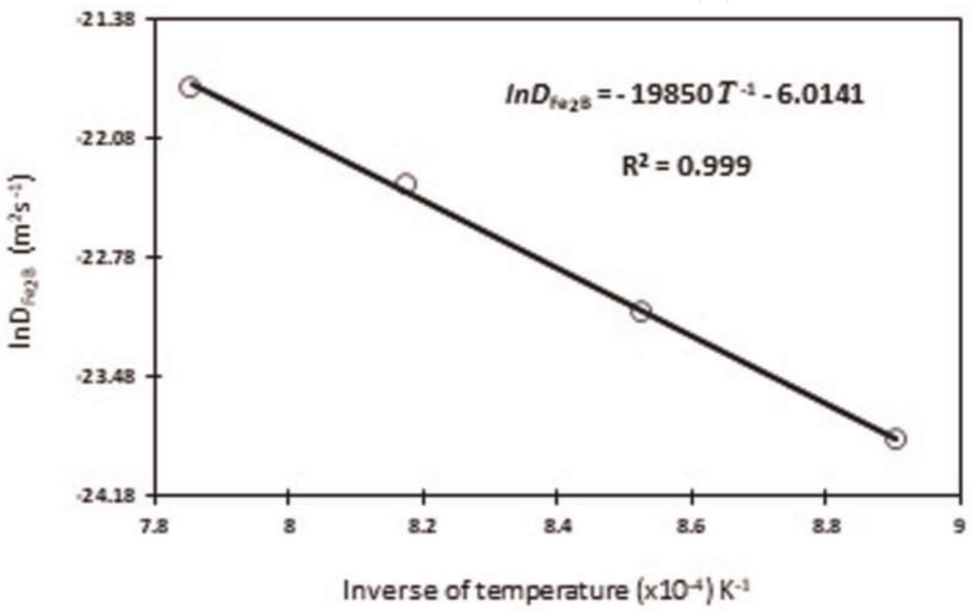

Figure 9.
Arrhenius relationship for boron diffusion coefficient (D_{Fe_2B}) through the Fe_2B layer obtained with the steady state diffusion model.

energy $\left(Q_{Fe_2B} = 165.0329\ \ kJmol^{-1}\right)$ values are affected by the contact surface between the boriding medium and the substrate, as well as the chemical composition of the substrate [9, 10, 23–28].

1.3.4 Estimation of boron activation energy with non-steady state diffusion model

In **Table 2** provides the growth constants ($2k_{Fe_2B}$) at each temperature, and in **Table 3** provides the boron diffusion coefficients (D_{Fe_2B}), they were estimated numerically by the Newton-Raphson method from the Eq. (26).

The boron activation energy $\left(Q_{Fe_2B} = 164.999\ \ \text{kJ mol}^{-1}\right)$ and pre-exponential factor $\left(D_0 = 2.072 \times 10^{-3}\ \text{m}^2/\text{s}\right)$ can be calculated from the slopes and intercepts of the straight line shown in coordinate system: $\ln D_{Fe_2B}$ as a function of reciprocal boriding temperature, it is presented in **Figure 10**, in the same way as above.

The boron diffusion coefficient through Fe_2B layers was deducted by non-steady state diffusion model as:

$$D_{Fe_2B} = 2.072 \times 10^{-3} \exp\left(-164.999\, kJmol^{-1}/RT\right) \quad \left[\text{m}^2\text{s}^{-1}\right]. \tag{28}$$

Temperature (K)	Type of layer	$\left(\frac{C_{up}^{Fe_2B}+C_{low}^{Fe_2B}-2C_0}{4}\right)(2k_{Fe_2B})^{1/2} = \sqrt{\frac{D_{Fe_2B}}{\pi}}\frac{C_{up}^{Fe_2B}-C_{low}^{Fe_2B}}{erf\left(\sqrt{\frac{k_{Fe_2B}}{2D_{Fe_2B}}}\right)}\exp\left(-\frac{k_{Fe_2B}}{2D_{Fe_2B}}\right)$ Eq. (26) ($m^2\ s^{-1}$)
1123	Fe_2B	4.362×10^{-11}
1173		9.174×10^{-11}
1223		1.933×10^{-10}
1273		3.433×10^{-10}

Table 3.
The boron diffusion coefficients (D_{Fe_2B}) as a function of boriding temperature.

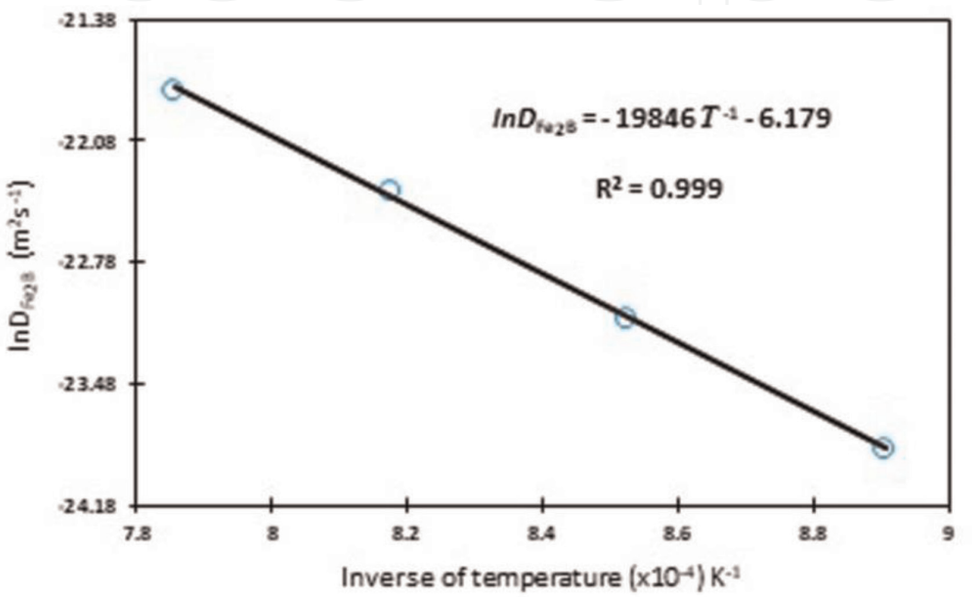

Figure 10.
Arrhenius relationship for boron diffusion coefficient (D_{Fe_2B}) through the Fe_2B layer obtained with the non-steady state diffusion model in on dimension.

1.3.5 The two diffusion models

In this section we want to illustrate the differences between the two diffusion models have been used to describe the growth kinetics of boride layers. It is noticed that the estimated values of boron activation energy $\left(Q_{Fe_2B} = 165.0\ kJmol^{-1}\right)$ for AISI 12L14 steel by steady state (see Eq. (27)) and non-steady state (see Eq. (28)), is exactly the same value for both diffusion models. Likewise, the estimated values of pre-exponential factor by steady state $\left(D_0 = 2.444 \times 10^{-3}\ m^2/s\right)$ and non-steady state $\left(D_0 = 2.072 \times 10^{-3}\ m^2/s\right)$, there is a small variation. To find out how this similarity is possible in the diffusion coefficients obtained by two different models, we first focus our attention on Eq. (23). The error function $erf\left(\sqrt{k_{Fe_2B}/2D_{Fe_2B}}\right)$ is a monotonically increasing odd function of $\sqrt{k_{Fe_2B}/2D_{Fe_2B}}$. Its Maclaurin series (for small $\sqrt{k_{Fe_2B}/2D_{Fe_2B}}$) is given by [29]:

$$erf\left(\sqrt{k_{Fe_2B}/2D_{Fe_2B}}\right) = \frac{2}{\sqrt{\pi}}\left(\sqrt{k_{Fe_2B}/2D_{Fe_2B}} - \frac{\left(\sqrt{k_{Fe_2B}/2D_{Fe_2B}}\right)^3}{3 \cdot 1!} + \frac{\left(\sqrt{k_{Fe_2B}/2D_{Fe_2B}}\right)^5}{5 \cdot 2!} - \cdots\right). \tag{29}$$

According to the numerical value of the $\sqrt{k_{Fe_2B}/2D_{Fe_2B}}$, Eq. (29) can be rewritten as:

$$erf\left(\sqrt{k_{Fe_2B}/2D_{Fe_2B}}\right) = 2\sqrt{k_{Fe_2B}/2D_{Fe_2B}\pi}. \tag{30}$$

Similarly for the real exponential function $\exp\left(-k_{Fe_2B}/2D_{Fe_2B}\right) : \mathbb{R} \to \mathbb{R}$ can be characterized in a variety of equivalent ways. Most commonly, it is defined by the following power series [30]:

$$exp\left(-k_{Fe_2B}/2D_{Fe_2B}\right) = 1 - k_{Fe_2B}/2D_{Fe_2B} + \left(-k_{Fe_2B}/2D_{Fe_2B}\right)^2/2! + \left(-k_{Fe_2B}/2D_{Fe_2B}\right)^3/3! + \cdots. \tag{31}$$

Thus, Eq. (31) can be written as:

$$exp\left(-k_{Fe_2B}/2D_{Fe_2B}\right) = 1. \tag{32}$$

By substituting the Eqs. (30) and (32) into Eq. (26), we have

$$\left(\frac{C_{up}^{Fe_2B} + C_{low}^{Fe_2B} - 2C_0}{4}\right)\left(2k_{Fe_2B}\right)^{1/2} = \sqrt{\frac{D_{Fe_2B}}{\pi}}\frac{C_{up}^{Fe_2B} - C_{low}^{Fe_2B}}{2\sqrt{\frac{k_{Fe_2B}}{2D_{Fe_2B}\pi}}}(1), \tag{33}$$

$$D_{Fe_2B} = \frac{1}{2}\left(\frac{C_{up}^{Fe_2B} + C_{low}^{Fe_2B} - 2C_0}{C_{up}^{Fe_2B} - C_{low}^{Fe_2B}}\right)k_{Fe_2B}. \tag{34}$$

The result obtained by Eq. (34) is the same as that obtained in Eq. (21) estimated by steady state diffusion model. The result from the Eq. (21) would appear to imply that the non-steady state diffusion model is superior to the steady state diffusion model and so should always be used. However, in many interesting cases the models are equivalent.

1.4 Fe_2B layer's thicknesses

The estimation of the Fe_2B layers' thicknesses can be determined through the Eqs. (35) and (36).

- Steady state diffusion model

$$\mathrm{v} = \sqrt{\left(3.33 \times 10^{-3}\right)\left(2.444 \times 10^{-3}\right)\exp\left(-\frac{165.0329\ \mathrm{kJ\ mol^{-1}}}{RT}\right)t} \quad [\mathrm{m}], \tag{35}$$

- Non-steady state diffusion model

$$\mathrm{v} = \sqrt{\left(3.33 \times 10^{-3}\right)\left(2.072 \times 10^{-3}\right)\exp\left(-\frac{164.999\ \mathrm{kJ\ mol^{-1}}}{RT}\right)t} \quad [\mathrm{m}], \tag{36}$$

Hence, Eqs. (35) and (36) can be used to estimate the optimum boride layer thicknesses for different borided ferrous materials.

2. Conclusions

The following conclusions can be drawn from the present study:

- Two simple kinetic models were proposed for estimating the boron diffusion coefficient in Fe_2B (steady state and non-steady state).
- A value of activation energy for AISI 12L14 steel was estimated as 165.0 kJ mol^{-1}.
- Two useful equations were derived for predicting the Fe_2B layer thickness as a function of boriding parameters (time and temperature).

Finally, these diffusion models are in general not identical, but are equivalent models, and this fact can be used as a tool to optimize the boriding parameters to produce boride layers with sufficient thicknesses that meet the requirements during service life.

Acknowledgements

The work described in this paper was supported by a grant of National Council of Science and Technology (CONACyT) and PRODEP México.

Conflict of interest

The author declares that there is no conflict of interests regarding the publication of this paper.

Nomenclature

v	boride layer thickness (m).
v_0	is a thin layer with a thickness of ≈ 5 nm that formed during the nucleation stage.
k_{Fe_2B}	rate constant in the Fe_2B phase (m^2/s).
t_v	effective growth time of the Fe_2B layer (s).
t	treatment time (s).
$t_0^{Fe_2B}$	boride incubation time (s).
$C_{up}^{Fe_2B}$	upper limit of boron content in Fe_2B (= 60×10^3 mol/m^3).
$C_{low}^{Fe_2B}$	lower limit of boron content in Fe_2B (= 59.8×10^3 mol/m^3).
C_0	terminal solubility of the interstitial solute (≈ 0 mol/m^3).
$C_{Fe_2B}[x(t),t]$	boron concentration profile (≈0 mol/m^3).
D_{Fe_2B}	boron diffusion coefficient (m^2/s).

IntechOpen

Author details

Martín Ortiz Domínguez
Autonomous University of Hidalgo State-Higher School of Ciudad Sahagún, Ciudad Sahagún, Hidalgo, México

*Address all correspondence to: martin_ortiz@uaeh.edu.mx

References

[1] Wahl G. Boronizing, a method for the production of hard surfaces for extreme wear. Durferrit-Technical Information. Reprint from VDI-Z117. Germany; 1975. pp. 785-789

[2] Graf von Matuschka A. Boronizing. 1st ed. Munich: Carl Hanser Verlag; 1980

[3] Davis JR. Surface Hardening of Steels Understanding the Basics. USA: ASM International; 2002. pp. 213-223

[4] Singhal SC. A hard diffusion boride coating for ferrous materials. Thin Solid Films. 1977;**45**:321-329

[5] Genel K, Ozbek I, Bindal C. Kinetics of boriding of AISI W1 steel. Materials Science and Engineering. 2003;**A347**: 311-314. DOI: 10.1016/S0921-5093(02) 00607-X

[6] Yapar U, Arısoy CF, Basman G, Yesilcubuk SA, Sesen MK. Influence of boronizing on mechanical properties of En-C35e steel. Key Engineering Materials. 2004;**264-268**:633-636. DOI: 10.4028/www.scientific.net/ KEM.264-268.629

[7] Fichtl W. Boronizing and its practical application. Revue Internationale des Hautes Températures. 1980;**17**:33-43. DOI: 10.1016/0261-3069(81)90034-0

[8] Campos-Silva I, Ortiz-Domínguez M, López-Perrusquia N, Meneses-Amador A, Escobar-Galindo R, Martínez-Trinidad J. Characterization of AISI 4140 borided steels. Applied Surface Science. 2010;**256**:2372-2379. DOI: 10.1016/j.apsusc.2009.10.070

[9] Kulka M, Makuch N, Pertek A, Maldzinski L. Simulation of the growth kinetics of boride layers formed on Fe during gas boriding in H_2-BCl_3 atmosphere. Journal of Solid State Chemistry. 2013;**199**:196-203. DOI: 10.1016/j.jssc.2012.12.029

[10] Brakman CM, Gommers AWJ, Mittemeijer EJ. Boriding Fe and Fe—C, Fe—Cr, and Fe—Ni alloys; boride-layer growth kinetics. Journal of Materials Research. 1989;**4**:1354-1370. DOI: 10.1557/JMR.1989.1354

[11] Yu LG, Chen XJ, Khor KA, Sundararajan G. FeB/Fe_2B phase transformation during SPS pack-boriding: Boride layer growth kinetics. Acta Materialia. 2005;**53**:2361-2368. DOI: 10.1016/j.actamat.2005.01.043

[12] Massalski TB. Binary Alloy Phase Diagrams. Materials Park, Ohio, USA: ASM International; 1990. p. 280. DOI: 10.1002/adma.19910031215

[13] Okamoto H. B—Fe (boron-iron). Journal of Phase Equilibria and Diffusion. 2004;**25**:297-298. DOI: 10.1007/s11669-004-0128-3

[14] Dybkov VI. Reaction Diffusion and Solid State Chemical Kinetics. Switzerland-UK-USA: Trans Tech Publications; 2010. p. 7. DOI: 10.4028/ www.scientific.net/MSFo.67-68

[15] Jost W. Diffusion in Solids, Liquids, Gases. New York: Academic Press Inc; 1960. pp. 69-72. DOI: 10.1002/ ange.19530651912

[16] Shewmon P. Diffusion in Solids. USA: Minerals Metals and Materials Society; 1989. p. 40

[17] Porter DA, Easterling KE. Phase Transformations in Metals and Alloys. London: Chapman and Hall; 1981. p. 105

[18] Martini C, Palombarini G, Carbucicchio M. Mechanism of thermochemical growth of iron borides on iron. Journal of Materials Science.

2004;**39**:933-937. DOI: 10.1023/B:JMSC.0000012924.74578.87

[19] Palombarini G, Carbucicchio M. Growth of boride coatings on iron. Journal of Materials Science Letters. 1987;**6**:415-416. DOI: 10.1007/BF01756781

[20] Ortiz Domínguez M. Contribución de la Modelación Matemática en el Tratamiento Termoquímico de Borurización [thesis]. México: SEPI-ESIME from the Instituto Politécnico Nacional; 2013

[21] Campos-Silva I, Bravo-Bárcenas D, Meneses-Amador A, Ortiz-Dominguez M, Cimenoglu H, Figueroa-López U, et al. Growth kinetics and mechanical properties of boride layers formed at the surface of the ASTM F-75 biomedical alloy. Surface and Coatings Technology. 2013;**237**:402-414. DOI: 10.1016/j.surfcoat.2013.06.083

[22] Campos-Silva I, Ortiz-Domínguez M, Bravo-Bárcenas O, Doñu-Ruiz MA, Bravo-Bárcenas D, Tapia-Quintero C, et al. Formation and kinetics of FeB/Fe_2B layers and diffusion zone at the surface of AISI 316 borided steels. Surface and Coatings Technology. 2010;**205**:403-412. DOI: 10.1016/j.surfcoat.2010.06.068

[23] Eyre TS. Effect of boronising on friction and wear of ferrous metals. Wear. 1975;**34**(3):383-397. DOI: 10.1016/0043-1648(75)90105-2

[24] Dukarevich IS, Mozharov MV, Shigarev AS. Redistribution of elements in boride coatings. Metallovedenie Termicheskaya i Obrabotka Metallov. 1973;(2):164-166. DOI: 10.1007/BF00679753

[25] Elias-Espinosa M, Ortiz-Domínguez M, Keddam M, Flores-Rentería MA, Damián-Mejía O, Zuno-Silva J, et al. Growth kinetics of the Fe_2B layers and adhesion on Armco iron substrate. Journal of Materials Engineering and Performance. 2014;**23**:2943-2952. DOI: 10.1007/s11665-014-1052-2

[26] Ortiz-Domínguez M, Keddam M, Elias-Espinosa M, Damián-Mejía O, Flores-Rentería MA, Arenas-Flores A, et al. Investigation of boriding kinetics of AISI D2 steel. Surface Engineering. 2014;**30**:490-497. DOI: 10.1179/1743294414Y.0000000273

[27] Ortiz-Domínguez M, Flores-Rentería MA, Keddam M, Elias-Espinosa M, Damián-Mejía O, Aldana-González JI, et al. Simulation of growth kinetics of Fe_2B layers formed on gray cast iron during the powder-pack boriding. Materiali in Tehnologije/Materials and Technology. 2014;**48**(6):905-916. Available from: http://mit.imt.si/Revija/izvodi/mit146/ortiz.pdf

[28] Campos-Silva I, Ortiz-Domínguez M, Tapia-Quintero C, Rodriguez-Castro G, Jimenez-Reyes MY, Chavez-Gutierrez E. Kinetics and boron diffusion in the FeB/Fe_2B layers formed at the surface of borided high-alloy steel. Journal of Materials Engineering and Performance. 2012;**21**:1714-1723. DOI: 10.1007/s11665-011-0088-9

[29] Ferraro G. The Rise and Development of the Theory of Series up to the Early 1820s. Denmark: Springer; 2008. pp. 147-149. DOI: 10.1007/978-0-387-73468-2

[30] Rubin W. Real and Complex Analysis. USA: McGraw-Hill; 1987. p. 1. https://59clc.files.wordpress.com/2011/01/real-and-complex-analysis.pdf